ICAS-88-3.4.4

QUADRILATERAL COONS SURFACE SHELL FINITE ELEMENT WITH DISCRETE PRINCIPAL CURVATURE LINES

T. Q. Ye and Yuerang Zhao
Northwestern Polytechnical University
Xi'an, Shaanxi
The People's Republic of China

Abstract

A new 48 degree-of-freedom quadrilateral thin shell finite element has been developed in this paper. B-spline Coons surfaces are used to model the middle surface of shells. The method of "discrete principal curvatures" is presented. This thin elastic shell finite element can be applied to analyze the shells of arbitrary shape which are encountered in structures of modern aircrafts and aerospace vehicles.Hence, the finite element analysis of thin shells can work with the computer aided design system. Numerical results show the efficiency of this finite element.

Introduction

The analyses of shells of arbitrary shape have significant practical interest for the aircraft and spacecraft structural design. The application of the finite element method to analyze the shell structures of arbitrary shape requires accurate representation of the shell geometry[1]. For the geometric description of arbitrary shell surfaces, Wu and Abel use a modified lofting method in which sectional curves are represented by a uniform B-spline and the surface is interpolated between sections by cardinal splines[2]. Moore and Yang developed a quadrilateral thin elastic shell finite element using variable-order polynomial functions and rational B-spline functions to model the shell middle surface. The displacement functions are that of bicubic Hermitian polynomials. The element has been used for linear and geometrically nonlinear analysis[3],[4]. Eberhardsteiner and Mang introduced the concept of "discrete orthogonalization of parameter lines" for the finite element analysis of thin shells[5].

It is known that for the shells with arbitrary shape the curvilinear system of reference provided by the CAD system or finite element mesh generation, or even the orthogonal lines, are not necessarily the principal curvature lines. However, most of shell theories are based on the assumption that the parametric lines are identical to the lines of principal curvatures. In order to circumvent above inconsistency, a technique of transformation of the curvilinear coordinate lines into the discrete principal curvatures has been developed. For present shell finite element the membrane displacement functions U and V are represented by reduced quartic polynomials, while the flexural displacement function W is the quintic polynomial. The rate of convergence in strain energy is of $O(h^6)$. To demonstrate the effeciency of this shell element, four numerical examples are presented in this paper. Results obtained are better than or in good agreement with the existing solutions by other shell finite elements or alternative methods.

SURFACE REPRESENTATION AND DISCRETE PRINCIPAL CURVATURES

There are various approaches for the surface representation which are developed on the basis of employing discrete data. The method presented in this paper for the finite element analysis is appropriate to any approach of surface representation. For instance, if we use the generalized Coons surface representation approach to model the shell surface[6]. The general form of this surface can be described as

$$r(\alpha_1,\alpha_2)=\sum_i \phi_i(\alpha_1)r(\alpha_1^i,\alpha_2)+ +\sum_j \phi_j(\alpha_2)r(\alpha_1,\alpha_2^j)-\sum_i\sum_j \phi_i(\alpha_1)\cdot \cdot\phi_j(\alpha_2)r(\alpha_1^i,\alpha_2^j) \quad (1)$$

where

$$\phi_i(\alpha_1^j)=\delta_{ij} \quad (2a)$$

$$\phi_j(\alpha_2^i)=\delta_{ji} \quad (2b)$$

are shape functions. Hermitian polynomials or splines are the common choices for these shape functions. Here we select the cubic B-splines as the interpolation functions. In Eq.(1), $r(\alpha_1,\alpha_2)$ is the vector-valued parametric representation of the shell surface in terms of two parametric variables of curvilinear coordinates α_1, α_2. Usually, the curvilinear coordinates α_1, α_2 for the surface representation in CAD system can not coincide with the principal curvature lines. But most of shell theories are established on the assumption that the curvilinear coordinates are the lines of principal curvature. For the shell surface of arbitrary shape, it is very cumbersome to find the lines of principal curvature. On the other hand, there is no need to construct "continuously" principal curvature lines for finite element formulation. For such formulation the metric and the curvature tensor only need to be evaluated at numerical integration points. Accordingly, it is sufficient to define the directions of principal curvature at discrete points. To express this concept, we use the term "discrete principal curvature" in contrast to the "continuously principal curvature lines"

Let X_1, X_2 and X_3 be the Cartesian coordinates, The shell surface can be described in the parametric form

$$X_i=f_i(\alpha_1,\alpha_2) \quad (3)$$

The coefficients of the first quadratic form of the surface are

$$A^2_{\xi\eta} = \frac{\partial X_k}{\partial \alpha_\xi}\frac{\partial X_k}{\partial \alpha_\eta}, \quad k = 1,2,3, \quad \xi, \eta = 1,2 \tag{4}$$

where Einstein's summation convention is used. Usually symbols E, F and G stand for above coefficients:

$$E = A^2_{11}, \quad F = A^2_{12}, \quad G = A^2_{22} \tag{5}$$

$A_{\xi\eta}$ are termed Lamé parameters.

The coeffients of the second quadratic form of the surface L, M and N are defined as

$$L = \frac{1}{\sqrt{EG - F^2}} \begin{vmatrix} \frac{\partial^2 X_1}{\partial \alpha_1^2} & \frac{\partial^2 X_2}{\partial \alpha_1^2} & \frac{\partial^2 X_3}{\partial \alpha_1^2} \\ \frac{\partial X_1}{\partial \alpha_1} & \frac{\partial X_2}{\partial \alpha_1} & \frac{\partial X_3}{\partial \alpha_1} \\ \frac{\partial X_1}{\partial \alpha_2} & \frac{\partial X_2}{\partial \alpha_2} & \frac{\partial X_3}{\partial \alpha_2} \end{vmatrix} \tag{6a}$$

$$M = \frac{1}{\sqrt{EG - F^2}} \begin{vmatrix} \frac{\partial^2 X_1}{\partial \alpha_1 \partial \alpha_2} & \frac{\partial^2 X_2}{\partial \alpha_1 \partial \alpha_2} & \frac{\partial^2 X_3}{\partial \alpha_1 \partial \alpha_2} \\ \frac{\partial X_1}{\partial \alpha_1} & \frac{\partial X_2}{\partial \alpha_1} & \frac{\partial X_3}{\partial \alpha_1} \\ \frac{\partial X_1}{\partial \alpha_2} & \frac{\partial X_2}{\partial \alpha_2} & \frac{\partial X_3}{\partial \alpha_2} \end{vmatrix} \tag{6b}$$

$$N = \frac{1}{\sqrt{EG - F^2}} \begin{vmatrix} \frac{\partial^2 X_1}{\partial \alpha_2^2} & \frac{\partial^2 X_2}{\partial \alpha_2^2} & \frac{\partial^2 X_3}{\partial \alpha_2^2} \\ \frac{\partial X_1}{\partial \alpha_1} & \frac{\partial X_2}{\partial \alpha_1} & \frac{\partial X_3}{\partial \alpha_1} \\ \frac{\partial X_1}{\partial \alpha_2} & \frac{\partial X_2}{\partial \alpha_2} & \frac{\partial X_3}{\partial \alpha_2} \end{vmatrix} \tag{6c}$$

The homogeneous system of equations for the unknown principal directions $d\alpha_1$ and $d\alpha_2$ is

$$(L + KE)d\alpha_1 + (M + KF)d\alpha_2 = 0 \tag{7a}$$

$$(M + KF)d\alpha_1 + (N + KG)d\alpha_2 = 0 \tag{7b}$$

The principal curvatures K_1 and K_2 than can be determined by solving the following equation

$$(EG - F^2) K^2 + (NE + LG - 2MF) K + + (LN - M^2) = 0 \tag{8}$$

Substitution of the principal curvatures K_1 and K_2 into whichever of Eqs. (5), for example into (5a), yields two principal directions

$$B_1 = \left(\frac{d\alpha_2}{d\alpha_1}\right)_1 = -\frac{L + K_1E}{M + K_1F} \tag{9a}$$

$$B_2 = \left(\frac{d\alpha_2}{d\alpha_1}\right)_2 = -\frac{L + K_2E}{M + K_2E} \tag{9b}$$

Let α'_1 and α'_2 be the coordinates of principal curvature, e'_1 and e'_2 —— the unit tangent vectors to the coordinate lines α'_1 = const. and α'_2 = const. respectively. e'_3 —— the unit normal which is perpendicular to the tangent plane. If the e_1 and e_2 indicate the unit tangent vectors to α_1 = const. and α_2 = const. respectively. The relationships connecting the two sets of unit tangent vector are written as

$$e'_1 = (e_1 + B_1e_2)/\sqrt{1 + B_1^2 + 2B_1\cos\theta} \tag{10a}$$

$$e'_2 = (e_1 + B_2e_2)/\sqrt{1 + B_2^2 + 2B_2\cos\theta} \tag{10b}$$

$$e'_3 = e_3 \tag{10c}$$

where $\cos\theta = F / \sqrt{EG}$ (10d)

The partial derivatives, which are useful for the chain-rule of differentiation, are given as follows

$$\frac{\partial\alpha_1}{\partial\alpha'_1} = (\sqrt{1 + B_1^2 + 2B_1\cos\theta})^{-1} \tag{11a}$$

$$\frac{\partial\alpha_2}{\partial\alpha'_1} = (\sqrt{1 + B_1^{-2} + 2B_1^{-1}\cos\theta})^{-1} \tag{11b}$$

$$\frac{\partial\alpha_1}{\partial\alpha'_2} = (\sqrt{1 + B_2^{-2} + 2B_2^{-1}\cos\theta})^{-1} \tag{11c}$$

$$\frac{\partial\alpha_2}{\partial\alpha'_2} = (\sqrt{1 + B_2^2 + 2B_2\cos\theta})^{-1} \tag{11d}$$

Applying the chain-rule of differentiation and using equations (11) we can obtain the Lamé parameters in the coordinates of principal curvature at discrete points.

The differentiation of Lamé parameters with respect to α'_i can be calculated approximately. If at the point (α_1, α_2) there is an increment $\Delta\alpha'_1$ in the direction of α'_1, thus we have

$$\Delta\alpha_1 = \Delta\alpha'_1 \frac{\partial\alpha_1}{\partial\alpha'_1} \tag{12a}$$

$$\Delta\alpha_2 = \Delta\alpha'_1 \frac{\partial\alpha_2}{\partial\alpha'_1} \tag{12b}$$

By virtue of Eqs. (12), the differentiation of Lamé parameters are then evaluated, for example, as follows

$$\frac{\partial A'}{\partial\alpha'_1} = \left[A'_1(\alpha_1 + \Delta\alpha_1, \alpha_2 + \Delta\alpha_2) - A'_1(\alpha_1, \alpha_2) \right] / \Delta\alpha'_1 \tag{13}$$

Similarly, we can calculated the other differentiations in the same way.

FINITE ELEMENT FORMULATIONS

The strain energy for elastic thin shell finite element is given by combining the membrane and the flexure portions

$$U_s = \frac{Eh}{2(1-\nu^2)} \int_\Omega \left(\varepsilon_1^2 + \varepsilon_2^2 + 2\nu\varepsilon_1\varepsilon_2 + \frac{1-\nu}{2}\omega^2 \right) d\Omega + \frac{Eh^3}{24(1-\nu^2)} \int_\Omega \left(\chi_1^2 + \chi_1^2 + 2\nu\chi_1\chi_2 + \frac{1-\nu}{2}\tau^2 \right) d\Omega \tag{14}$$

Novozhilov's thin shell theory is applied in this paper. The strain--displacement relations can be found in Ref. 7.

The quadrilateral thin shell finite element has four corner nodes, each of which has 12 d.o.f. with a total 48 d.o.f.. The membrane displacement functions are represented by reduced quartic polynomials, and a reduced 6th-order polynomial is chosen as the flexural displacement function W which is equivalent the complete quintic polynomial for the estimation of the rate of convergence.

NUMERICAL EXAMPLES

Four examples are presented to show the efficiency of the thin shell finite element developed in this paper. The B-spline Coons surfaces are used to describe the shell surface. Results obtained compare favourably with the exact solutions as well as finite element solutions by employing other shell finite elements.

Example 1. A barrel vault under self gravity load (Fig.1). Thickness of the shell t = 0.25 ft , E = 3.0 10^6 psi, ν = 0, self gravity load wt = 90 psi. Figure 2 shows the comparison of the present solution with the existing solutions.

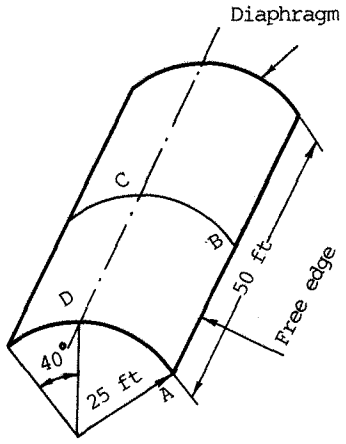

Figure 1. Barrel vault under self gravity load

Normal displacements of the barrel vault along the line BC (see Fig.1) are portrayed in Fig.3.

Example 2. A pinched cylindrical shell under two opposite concentrated loads. E = 10.5 10^6 psi, ν = 0.3125, load P = 100 lbs (Fig. 4). The normal displacement of the point C (see Fig. 4) is shown in Fig. 5. The results are compared with the exact solution , and the rate of convergence can be discovered. Figure 6 shows the normal displacement of the point B of pinched cylindrical shell. Above results are also listed in Table I .

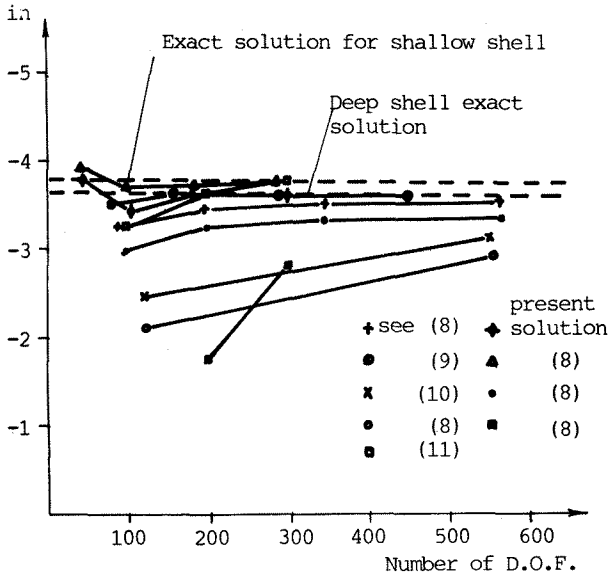

Figure 2. Numerical comparison— normal displacement of point B of the barrel vault

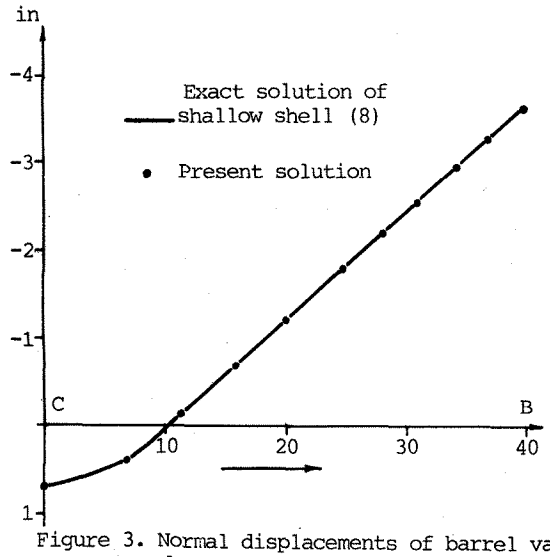

Figure 3. Normal displacements of barrel vault along the line BC

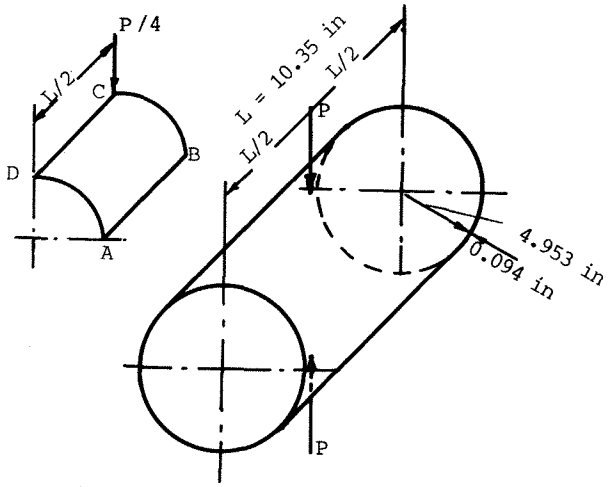

Figure 4. Pinched cylindrical shell under two opposite concentrated loads

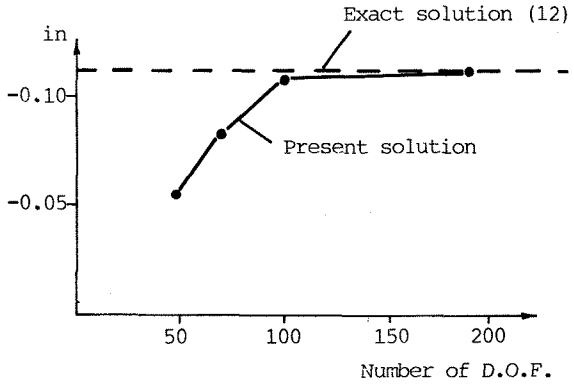

Figure 5. Normal displacement of the point C of pinched cylindrical shell

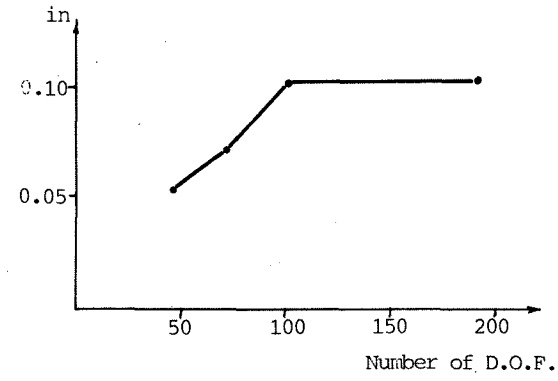

Figure 6. Normal displacement of the point B of pinched cylindrical shell

Table I

Mesh	Normal displacement of point C (W_C)				W_B
	Present solution	Cantin (12)	Ashwell and Sabir (15)	Thomas and Gallagher (16)	Present solution
1 x 1	-0.0565		-0.1040	-0.0048	0.0525
1 x 2	-0.0772				0.0737
1 x 4			-0.1106	-0.1107	
2 x 2	-0.1138	-0.0931	-0.1103		0.1044
3 x 3	-0.1139				0.1045
4 x 4		-0.1126	-0.1129		
6 x 6		-0.1137	-0.1135		
8 x 8		-0.1139	-0.1137		
10 x 10		-0.1139	-0.1137		

Example 3. A spherical cap under concentrated load. The spherical surface is described by the equation

$$X^2 + Y^2 + Z^2 = 100^2$$

A concentrated load of 100 lbs is applied at the center of the cap (Fig. 7). $E = 10^7$ psi , $\nu = 0.3$, the thickness of the shell t = 0.1 in. The results of calculation are shown in Table II and Figs. 8 and 9 which are compared with the analytical solutions and other finite element solutions.

Table II

Mesh	Present solution	Yang's F.E.M. solution (13)
1 x 1	-0.02521	-0.00991
2 x 1		-0.01859
2 x 2	-0.03556	-0.03595
2 x 3	-0.03785	-0.03690
2 x 4	-0.03860	-0.03747
3 x 3	-0.04007	-0.03867
4 x 4	-0.04008	
Analytical solution (See (13))	-0.03956	-0.03956

Example 4. A hyperbolic paraboloidal shell under uniform distributed load of 0.01 psi (Fig.10). Thickness of shell t = 0.8 in , ν =0.4 E = 28500 psi. The shell surface has the equation

$$Z = 0.004XY$$

Figure 11 shows the normal displacement of the center of the shell W_O . These results also are listed in Table III.which are compared with other finite element solutions. Figure 12 describe the normal displacements along the line EF of the shell.

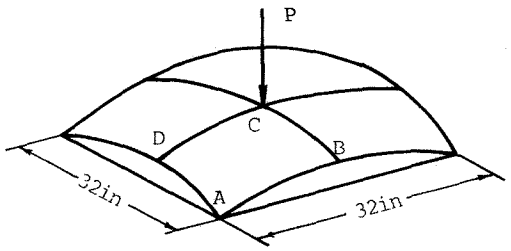

Figure 7. Spherical cap under concentrated load

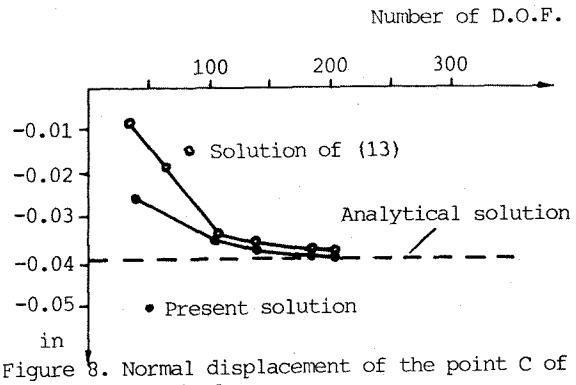

Figure 8. Normal displacement of the point C of spherical cap

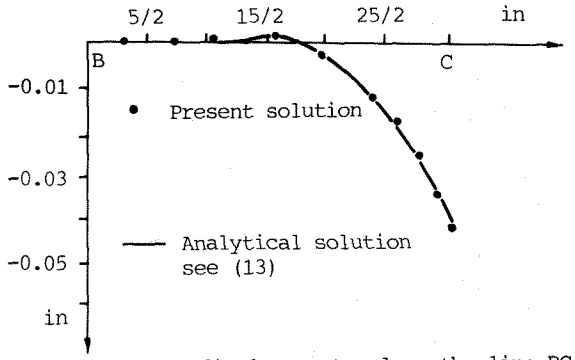

Figure 9. Normal displacements along the line BC of spherical cap

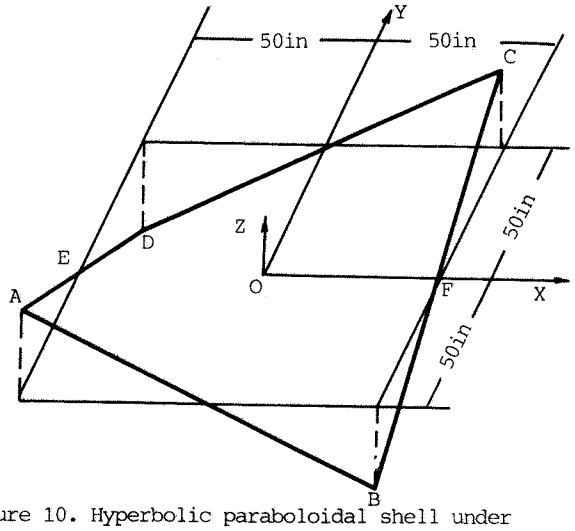

Figure 10. Hyperbolic paraboloidal shell under uniform load

Table III

Mesh	Present solution	Solution in (14)	Solution in (13)
2 x 2	-0.03327	-0.0408	-0.0459
4 x 4	-0.02468	-0.0288	-0.02472
6 x 6	-0.02453		-0.02465
8 x 8		-0.02457	

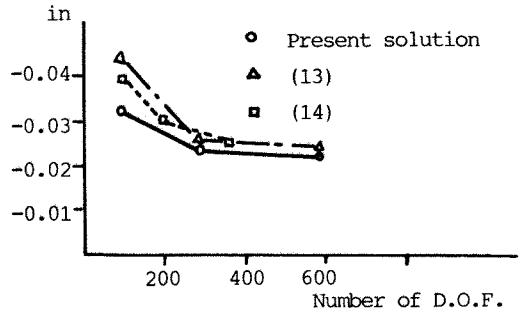

Figure 11. Normal displacement of the point o of hyperbolic paraboloidal shell

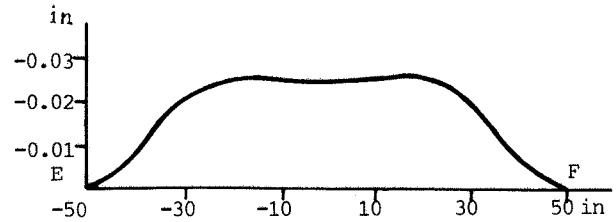

Figure 12. Normal displacements along the line EF of hyperbolic paraboloidal shell

CONCLUSIONS

The 48 degree-of-freedom quadrilateral Coons surface shell finite element has been developed in this paper which can be used to analyze shells of arbitrary shapes. This new finite element also has the advantage that it may be linked to the data bases of the CAD system for the aircraft and spacecraft design. By virtue of using more exact geometric description of shell surfaces and developing the concept of " discrete principal curvatures and by proper choosing the displacement function representations, this shell element possesses higher rate of convergence which can be observed in the numerical examples.

REFERENCES

1. Ashwell, D. G. and Gallagher, R. H., Ed. FINITE ELEMENTS FOR THIN SHELLS AND CURVED MEMBERS, Wiley, New York, 1976
2. Wu, Sheng-Chuan and Abel, J. F.,Representation and discretization of arbitrary surfaces for finite element shell analysis, Int. J. Num. Meth. Eng., Vol.14, 813-836, 1979.
3. Moore, C. J., and Yang, T. Y., A new 48 d.o.f. quadrilateral shell element with variable-order polynomial and rational B-spline geometries with rigid body modes, Int. J. Num. Meth. Eng., Vol. 20, 2121-2141, 1984.
4. Yang, T. Y. Moore, C. J. and Anderson, D. C., Geometrically nonlinear formulation of a 48 d.o.f. quadrilateral shell element with rational B-spline geometry, Int. J. Num. Meth. Eng., 317-328, 1985
5. Eberhardsteiner, J. and Mang, H. A., Discret orthogonalization of parameter lines on curved surfaces for finite element analysis of thin shells, Int. J. Num. Meth. Eng., Vol. 21, 837-851, 1985.
6. Gordon, W. J. and Hall, C. A. , Transfinite element methods: blending-function interpolation over arbitrary curved element domains, Num. Math., Vol. 21, 1973.
7. Novozhilov, V. V., THIN SHELL THEORY, Wolters-Noordhoff, Groningen, 1970
8. Ashwell, D. G., Strain elements with application to arches, rings and cylindrical shells, in Ref. 1.
9. Dawe, D. J., Some high-order elements for arches and shells, in Ref. 1.
10. Strickland, C. E. and Lodon, W. A., A doubly -curved triangular shell element, Proc. 2nd Conf. Matrix Meth. Struct. Mech., AFFDL-TR-68-150, Wright-Patterson Air Force Base, Ohio, 1968.
11. Cowper, G. R., Lindberg, G. M., and Olson, M. P., A shallow shell finite element of triangular shape, Int. J. of Sol. and Struct., Vol.6 1133-1156, 1970.
12. Cantin, G., Rigid body motions in curved finite elements, AIAA J. Vol. 8, No.7, 1970.

13. Yang, T. Y., High order rectangular shallow shell finite element, J. eng. Mech. Div. ASCE, Vol. 99, No. EM1, 1973
14. Connor, J. J., and Brebbia, C. A., Stiffness matrix for shallow rectangular shell element, J. Eng. Mech. Div. ASCE, Vol. 93 43-65, 1967.
15. Ashwell, D. G. and Sabir, A. B., A new cylindrical shell finite element based on simple independent strain functions, Int. J. Mech. Sci., Vol.14, 1972
16. Thomas, G. R., and Gallagher, R. H., A triangular element based on generalized potential energy concept, In. Ref.1.

ACKNOWLEDGEMENT

The authors acknowledge the support of this work by the Fund of the Natural Sciences of China.